www.czasopisma.pan.pl PAN POLSKA AKADEMIA NAUK www.journals.pan.pl

Arch. Metall. Mater. **65** (2020), 4, 1377-1383

DOI: 10.24425/amm.2020.133703

S. STĄPÓR[1*], M. GÓRNY[1], M. KAWALEC[1], B. GRACZ[1]

EFFECT OF VARIABLE MANGANESE CONTENT ON MICROSTRUCTURE OF Al-Cu ALLOYS

The presented access the influence of Mn content (0-0.94 wt.%) on the course of the cooling curves, phase transformation, macrostructure, and microstructure of Al-Cu alloys for three series: initial (Series I), with the addition of an AlTi master (Series II), and modified with AlTi5B1 (Series III). The maximum degree of undercooling ΔT was determined based on the cooling curves. The surface density of the grains (N_A) was determined and associated with the inverse of solidification interval $1/\Delta T_k$. Titanium (contained in the charge materials as well as the modifier) has a significant effect on the grinding of the primary grains in the tested alloys. A DSC thermal analysis allowed for the determination of phase transition temperatures under conditions close to equilibrium. For series II and III, the number of grains decreases above 0.2 wt.% Mn with a simultaneous increase in solidification interval $1/\Delta T_k$. The presence of Al_2Cu eutectics as well as the Cu-, Fe-, and Mn-containing phases in the examined samples was demonstrated using scanning electron microscopy.

Keywords: Al-Cu-Mn alloys, Microstructure, Macrostructure, DSC

1. Introduction

Al-Cu-Mn alloys are high-strength materials that are widely used in the aerospace and automotive industries [1,2]. This is due to their favorable properties at both ambient and elevated temperatures [1-3]. Compared to other alloys, these are distinguished by considerable strength and lightness [1,3]. High-quality Al-Cu-Mn alloys have excellent mechanical properties after T6-type heat treatment. Their tensile strength may then exceed 500 MPa and elongation 6.5% [4].

The properties of the materials are related to their microstructure, so it is very important to control it. Changes in the distribution and size of the phases significantly affect the strength parameters of the alloys [2]. The main alloying elements used in high-quality Al-Cu alloys (the 2xx groups, according to the Aluminum Association [AA]) are magnesium and manganese (among others) as well as elements that affect grain refinement (including titanium). As the main alloying element, copper affects on the strength and hardness of casting alloys [5]. The content of this element is within a range of 4-6 wt.% in these alloys. On the other hand, manganese is used in much smaller amounts (0.3-1.0 wt.%) [6]. The alloys owe their high strength to heat treatment (solution treatment and aging). As a result, a metastable θ' and T-phase ($Al_{20}Cu_2Mn_3$) are precipitated [3].

According to the literature [5], the influence of Mn on the mechanical properties of aluminum alloys shows that a manganese content above 0.5% prompts a strength-property increase without a loss in ductility. The advantage of using manganese as an additive is also its beneficial effect on corrosion resistance [5]. This element has a positive effect on strength properties at elevated temperatures as a result of the formation of the favorable $Al_{20}Cu_2Mn_3$ phase [7]. The presence of other elements (including Fe, Ni, or Si) in the 2xx-group alloys is an undesirable phenomenon. These elements combine with manganese to form phases that contribute to a reduction in its content in the metal matrix, weakening the mechanical properties of these alloys [7]. Iron is an element with a negative effect on Al-Cu alloys. This is mainly due to the shape of the phases that it forms [8,9]. Phases rich in iron (β-Fe) in plate form are more unfavorable than those occurring as compact phases or in the form of so-called Chinese writing [9].

The current literature data provides information on the topicality of the issue taken up in the research on the phase shaping and strengthening of the 2xx group alloys' [3,8,9] microporosity [4] and crystal growth restriction GRF (Growth Restriction Factor), among others [10,11].

Due to the great importance of favorable features as well as the possibility of using Al-Cu-Mn alloys in many industries, it is

[1] AGH UNIVERSITY OF SCIENCE AND TECHNOLOGY, FACULTY OF FOUNDRY ENGINEERING, 23 REYMONTA STR., 30-059 KRAKOW, POLAND

* Corresponding author: sylwiapaz@agh.edu.pl

© 2020. The Author(s). This is an open-access article distributed under the terms of the Creative Commons Attribution-NonCommercial License (CC BY-NC 4.0, https://creativecommons.org/licenses/by-nc/4.0/deed.en which permits the use, redistribution of the material in any medium or format, transforming and building upon the material, provided that the article is properly cited, the use is noncommercial, and no modifications or adaptations are made.

necessary to develop these alloys and conduct research that can improve those materials that are currently being used. The following research was conducted to identify the effect of Mn on the course of the cooling curves, macrostructure, and microstructure of Al-Cu alloys with the addition of variable manganese contents as well as the correlation of individual parameters.

2. Experimental procedure

The presented research included three melts. The liquid metal was melted in an induction furnace. Series I included the preparation of the base alloy. The furnace charge contained technically pure aluminum and an AlCu50 master alloy. An additional AlTi master alloy was introduced in Series II, while the AlTi5B1 modifier was used in Series III (0.2% in relation to the weight of the charge). AlMn75 was introduced in order to obtain a variable Mn content. A chill (PM mould – means metal form) was used for the tests, allowing us to obtain a roller-shaped casting with a diameter of 15 mm. The temperature of the metal mold during pouring was 250°C. The casting temperature was 750°C. To record the cooling curves, cups for a thermal analysis (mould S) were used (K-type thermocouple). These cups were connected to an Agilent 34970A digital recorder.

Table 1 shows the chemical composition for the individual samples carried out using a SPECTROMAXx emission spectrometer.

TABLE 1

Chemical composition of tested samples

Series	Determination of the Mn content	Element content, wt.%					
		Si	Fe	Cu	Mn	Ti	Al
I	A	0.04	0.07	4.96	**0.00**	0.01	Remainder
	B	0.04	0.07	5.07	**0.28**	0.01	Remainder
	C	0.04	0.07	5.07	**0.43**	0.01	Remainder
	D	0.04	0.08	4.81	**0.94**	0.00	Remainder
II	A	0.03	0.12	4.96	**0.00**	0.05	Remainder
	B	0.04	0.11	4.53	**0.24**	0.10	Remainder
	C	0.04	0.12	4.88	**0.39**	0.11	Remainder
	D	0.05	0.14	4.99	**0.94**	0.12	Remainder
III	A	0.08	0.10	4.62	**0.00**	0.12	Remainder
	B	0.07	0.11	4.86	**0.24**	0.13	Remainder
	C	0.06	0.10	4.28	**0.36**	0.16	Remainder
	D	0.07	0.11	4.69	**0.86**	0.16	Remainder

Samples for testing were cut from the S-casting and then ground and polished. In addition, the samples were electrolytically etched in a 5% HBF_4 solution using an electric current of 30 V for at least one minute. Then the average grain diameter and surface density of grains N_A (the planimetric method) was determined.

A Leica MEF4M optical microscope was used for the metallographic examination. Observations were carried out in polarized light on a Leica MZ6 stereomicroscope, while a scanning electron microscope (Jeol 5500LV) with an EDS system was used to check the composition of the occurring phases.

The research also included performing a DSC thermal analysis using a DSC Q20 differential calorimeter. The samples were melted and subsequently cooled in an argon atmosphere. A cooling and heating rate of 10°C/min was used within a range of 400-700°C.

3. Results and discussion

Thermal analysis

Fig. 1, 2, and 3 show the recorded cooling and crystallization curves in the α (Al) phase range that were used to determine the degree of undercooling ΔT.

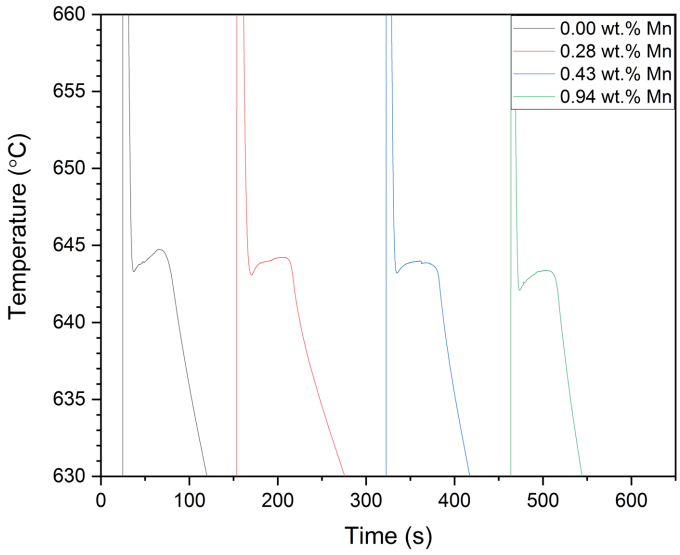

Fig. 1. Cooling curves for Series I – (unmodified alloy, trace Ti content)

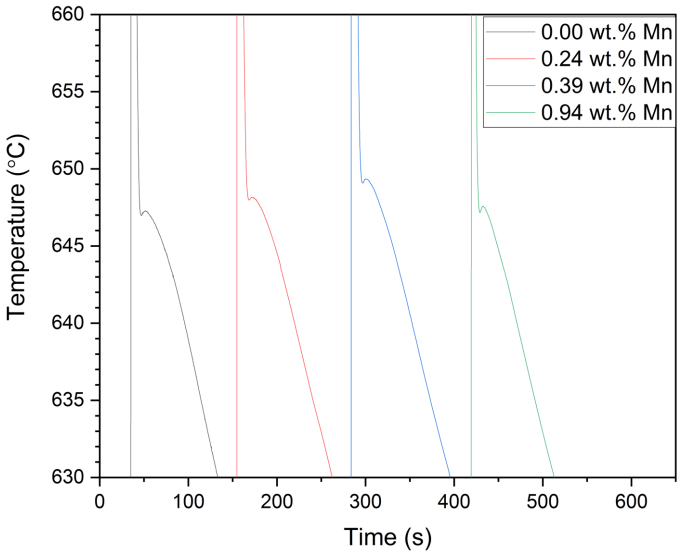

Fig. 2. Cooling curves for Series II (unmodified alloy, Ti content 0.1 wt.%)

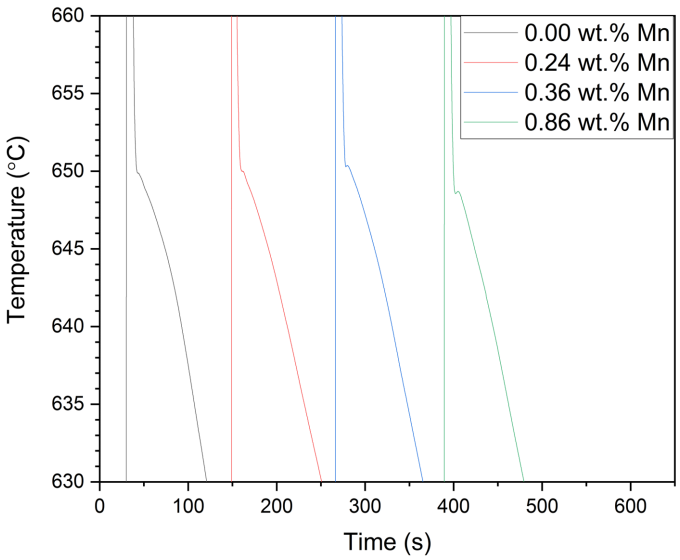

Fig. 3. Cooling curves for Series III (modified alloy, Ti content 0.1 wt.%)

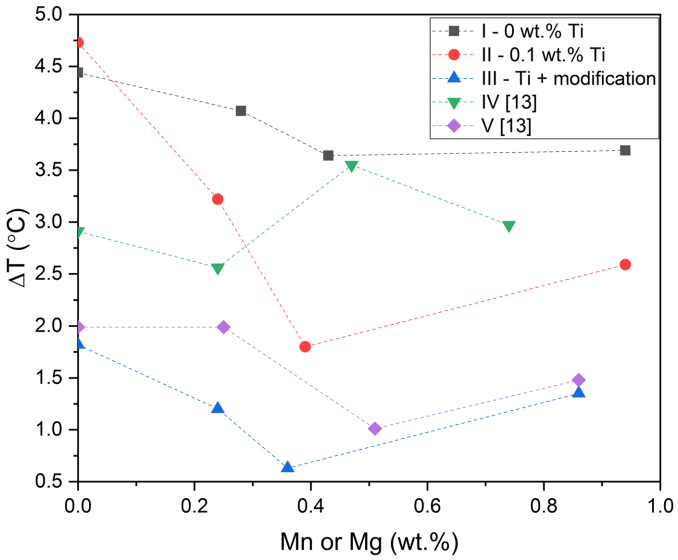

Fig. 4. Undercooling degree depending on manganese and magnesium contents. Al-Cu-Mn alloys: I – series with trace Ti content; II – series with 0.1 wt.% Ti content; III – series modified with Ti. Al-Cu-Mg alloys: IV – unmodified; V – modified

The maximum degree of undercooling ΔT was determined from Eq. (1), which captures the effect of the alloying additives on the equilibrium temperature of the crystallization of dendrite phase α(Al) [12]:

$$\Delta T = T_L - T_{\min} \tag{1}$$

where:

$$T_L = T_F + \bar{m}_L \bar{C}_L \tag{2}$$

$$\bar{m}_L = \sum_{i=1}^{n} \left(m_L^i C_L^i \right) / \bar{C}_L \tag{3}$$

$\bar{m}_L$ – average slope factor of liquidus line[1],
$\bar{C}_L$ – sum of all elements in liquid metal,
T_F – crystallization temperature for pure aluminum; $T_F = 660{,}45$°C,
T_L – equilibrium crystallization temperature of dendrite α (Al) phase,
$T_{\min}$ – minimum temperature at beginning of alloy crystallization,
m_L^i – slope factor of liquidus line of individual elements,
C_L^i – concentration of i – component.

The minimum temperature for each series was determined from digital data recorded during temperature measurement. The calculated values of the undercooling degree as a function of the variable content of Mn are illustrated in Figure 4.

The values of the maximum degree of undercooling ΔT decreases as the Mn content in the alloys increases (up to 0.4% Mn), followed by its increase to 0.9 wt.% Mn. For Series I (unmodified alloy, trace Ti content), the difference in the degree of undercooling is 0.8°C. For Series II (unmodified alloy, Ti content 0.1 wt.%), this is 2.93°C. For Series III (modified with AlTi5B1 master), the difference is 1.19°C. The addition of Ti at a level of about 0.1 wt.% in the Al-Cu-Mn alloy causes the greatest differences in the maximum degree of undercooling (within a range of 0-0.4 wt.% Mn). A further increase in Mn increases the maximum degree of undercooling. Based on literature data [13], it is worth noting (Fig. 4) that the action of magnesium is analogous to manganese in terms of reducing the maximum degree of undercooling as well as the occurrence of a minimum in the Mg = $f(\Delta T)$ system.

Literature data related to the degree of undercooling in Al-Cu alloys [14] shows that it increases in the initial series along with increasing copper content (Fig. 5). However, an inverse relationship is visible for the modified series. This effect

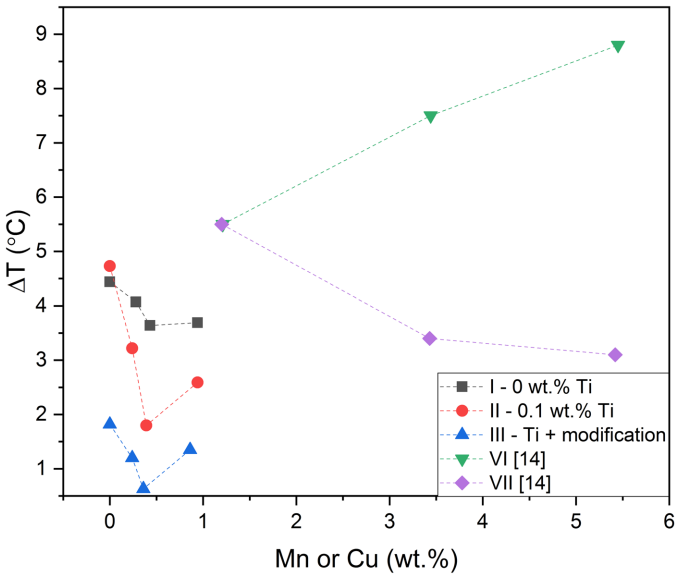

Fig. 5. Degree of undercooling depending on manganese and copper content. Al-Cu-Mn alloys: I – series with trace Ti content; II – series with 0.1 wt.% Ti content; III – series modified with Ti. Al-Cu alloys: VI – unmodified; VII – modified

[1] The average slope factor of the liquidus line was determined for the variable content of Mn and the average values of the contents of other elements in the respective melts.

should be explained by the segregation of copper into the liquid phase during crystallization. At higher copper contents, eutectic composition is achieved more quickly. Then, the eutectic crystallizes [14]. In the case of the unmodified alloy, this is associated with the phenomenon of grain growth inhibition (i.e. the GRF). In the case of a modified alloy, the modification treatment also works (which significantly reduces the degree of undercooling).

Metallographic examinations

Fig. 6 and 7 show examples of the macrostructures and microstructures of the tested Al-Cu-Mn alloys. A slight decrease in the number of dendritic cells was observed with increasing Mn content for each individual series. The surface fraction of eutectic slightly increases with the increase of manganese content.

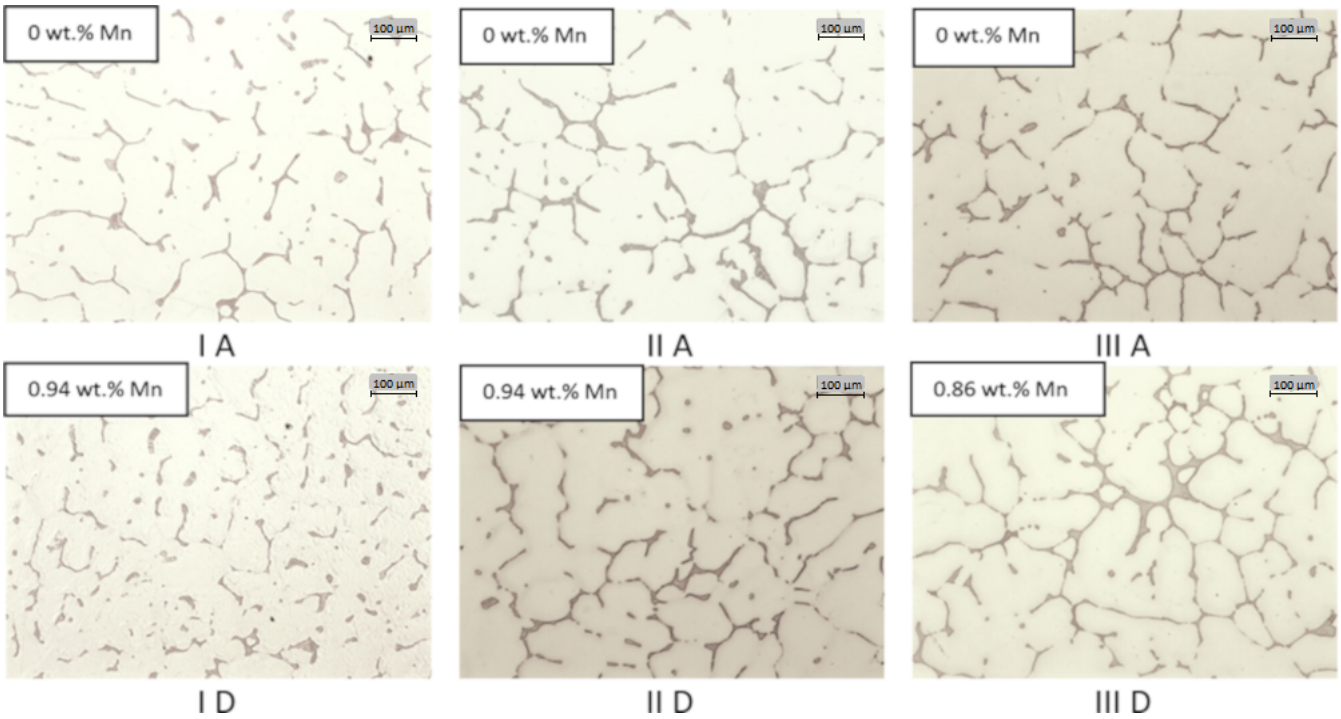

Fig. 6. Selected cast microstructures (mould S), 100× magnification, polished state. Al-Cu-Mn alloys: I – series with trace Ti content; II – series with 0.1 wt.% Ti content; III – series modified with Ti

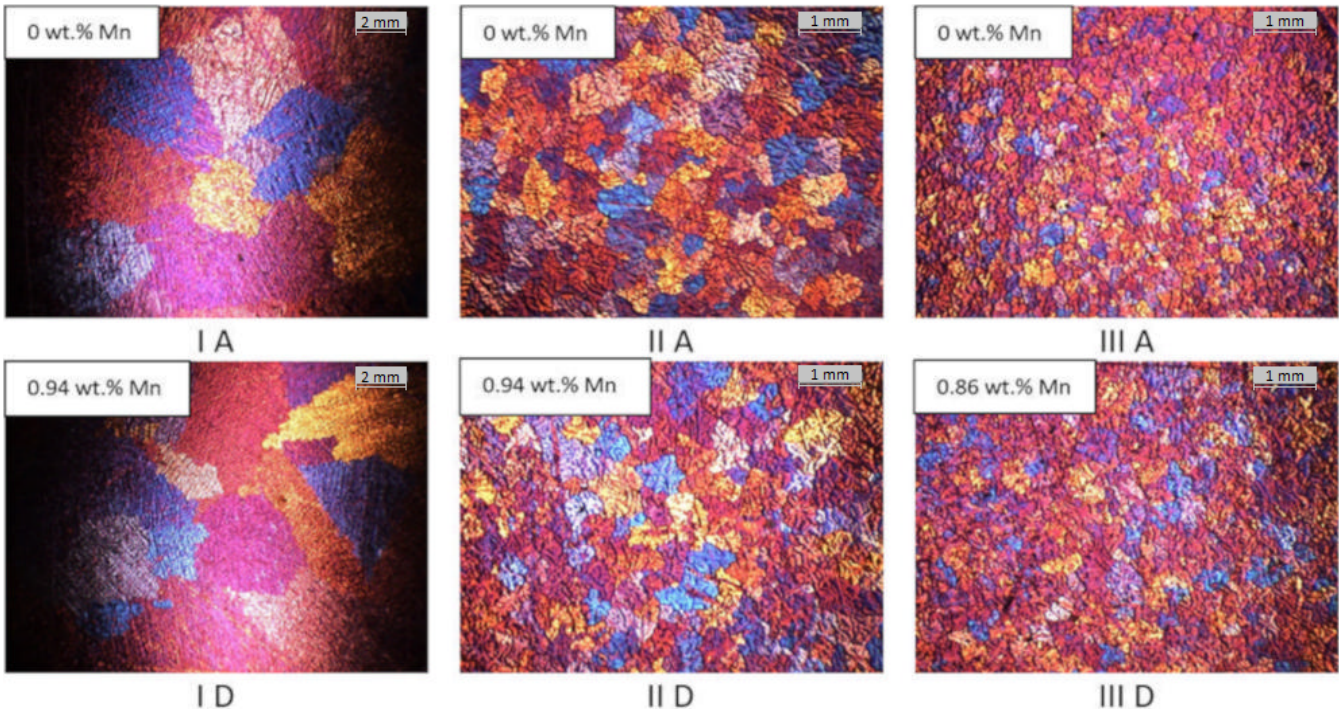

Fig. 7. Selected macrostructures of tested IA, ID alloys – 8x magnification, others – 20×, electrolytically etched. Al-Cu-Mn alloys: I – series with trace Ti content; II – series with 0.1 wt.% Ti content; III – series modified with Ti

The results of the surface density of the N_A grains as a function of Mn content are shown in Figure 8. With increasing amounts of manganese, the number of primary grains per unit of surface decreases. It has been observed that the addition of manganese slightly reduces the effectiveness of the modification procedure (Series III). The obtained results indicate that the optimal Mn content should be about 0.25% from the point of view of the maximum number of primary grains in the alloys tested. The studies have also shown that large differences in the grain sizes are visible between the Al-Cu-Mn alloy without Ti and that with about 0.1 wt.% Ti. On this basis, it has been shown that the addition of titanium comminutes the primary grains to a significant degree in the alloys tested. This fact confirms its high growth restriction factor, which indicates the great impact of titanium. The most grains per unit area were obtained for the modified Al-Cu-Mn alloy (Series III).

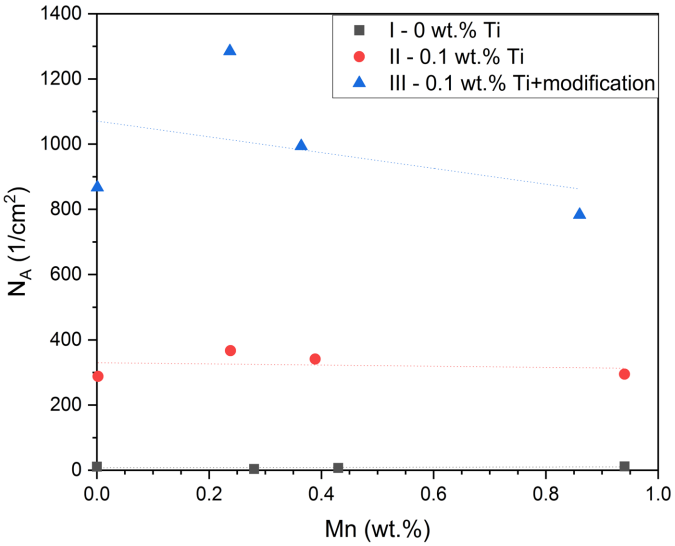

Fig. 8. Surface density of grains N_A depending on the manganese content

The GRF plays an important role in the microstructure-shaping process. Table 2 presents the values of $m(k-1)$ for the individual elements that allow for the calculation of the GRF [11]. The GRF depends on the concentration of a given element in the alloy and is determined by Eq. (4).

$$GRF = mc_0(k-1) \tag{4}$$

where:

c_0 – concentration of element in alloy,
m – slope of liquidus line,
k – partition coefficient.

Table 2 presents the values of $m(k-1)$ for the selected elements with respect to aluminum alloys.

The value of the GRF manganese growth restriction factor is very low. Ti has the highest value of this parameter. Fig. 8 shows that, due to the high GRF coefficient, Ti plays a significant and dominant role in grinding the primary grains for a given Mn content. The impact of manganese is much weaker due to its low GRF growth restriction factor.

TABLE 2

Values of $m(k-1)$ for selected elements [10]

Element	$m(k-1)$
Ti	245.6
Cu	2.8
Mn	0.1
Mg	3.0
Si	5.9

Figure 9 shows the dependence of the number of primary grains of phase α (Al) as a function of the degree of undercooling as well as the content of Mn in the alloy. The addition of about 0.4 wt.% of manganese causes a reduction in the degree of undercooling. Slight increase in the undercooling level was observed at a content of 0.9 wt.% Mn. It is worth noting that the action of manganese (0.4 wt.% Mn) in the unmodified alloy reduced the degree of undercooling to the level of the modified alloy ($\Delta T = 1 \div 2^{o}$C). The operation of titanium only extends the range of the degree of undercooling, while the modification treatment reduces it.

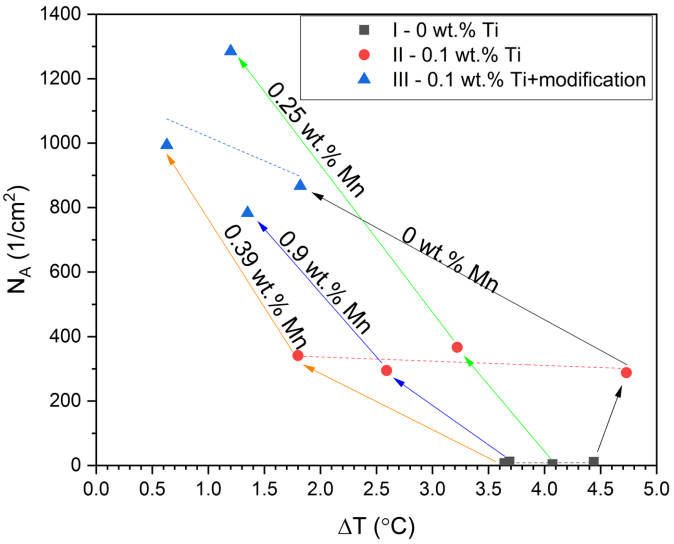

Fig. 9. Surface grain density N_A depending on degree of undercooling ΔT

Differential Scanning Calorimetry (DSC)

Based on the DSC thermal analysis, the characteristic temperatures were determined in a Universal Analysis. The obtained results are summarized in Table 3.

The solidification interval and limiting solubility depend on various factors that affect the physicochemical state and cooling rate. Commercial alloys contain alloying and trace elements that affect the crystallization process. This causes various transformations (eutectic, peritectic) as well as the formation of complex intermetallic phases. The solidification interval determined from the DSC analysis can be related to the grain size in the alloys tested. The obtained values of the inverse of the solidification interval are summarized in Figs. 10-12 depending on the Mn content, taking into account their variable physicochemical states (Series I-III).

TABLE 3

Characteristic temperatures determined from DSC charts: Series I – trace Ti content; Series II – Ti content of 0.1 wt.%; Series III – Ti + modification

Series		Temperatures determined from DSC charts		$1/\Delta T_k \times 10^2$ °C^{-1}
		Beginning of solidification, T_α, °C	End of solidification, T_S, °C	
I	A	633.47	532.47	0.990
	B	634.5	529.75	0.955
	C	635.86	528.68	0.933
	D	637.64	529.75	0.927
II	A	643.3	529.66	0.880
	B	644.22	529.65	0.873
	C	645.5	529.4	0.861
	D	645.24	530.89	0.875
III	A	645.17	531.2	0.877
	B	645.99	529.03	0.855
	C	644.32	527.2	0.854
	D	642.81	526.54	0.860

ΔT_k – solidification interval, where $\Delta T_k = T_\alpha - T_S$

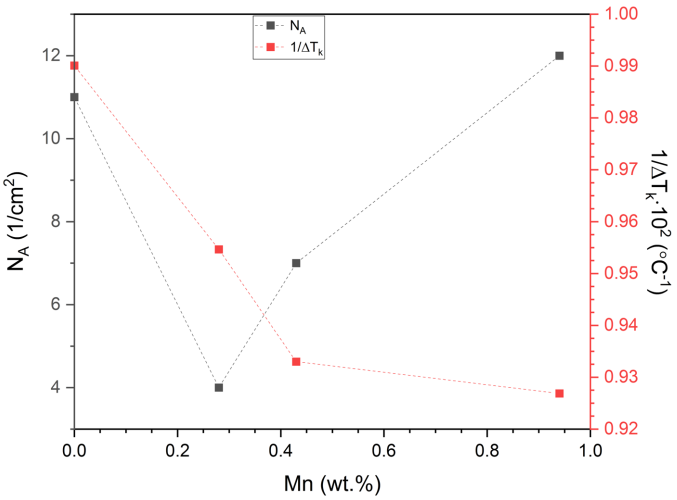

Fig. 10. Number of grains per unit area N_A and $1/\Delta T_k$ as function of variable Mn content for Series I (unmodified alloy, trace Ti content)

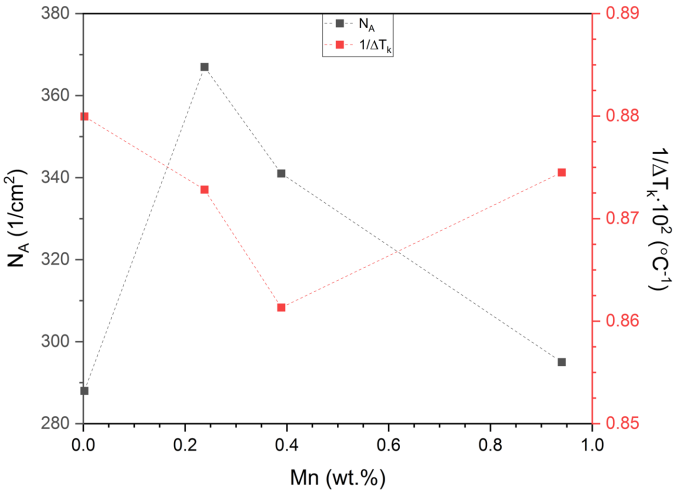

Fig. 11. Number of grains per unit area N_A and $1/\Delta T_k$ as function of variable Mn content for Series II (unmodified alloy, Ti content of 0.1 wt.%)

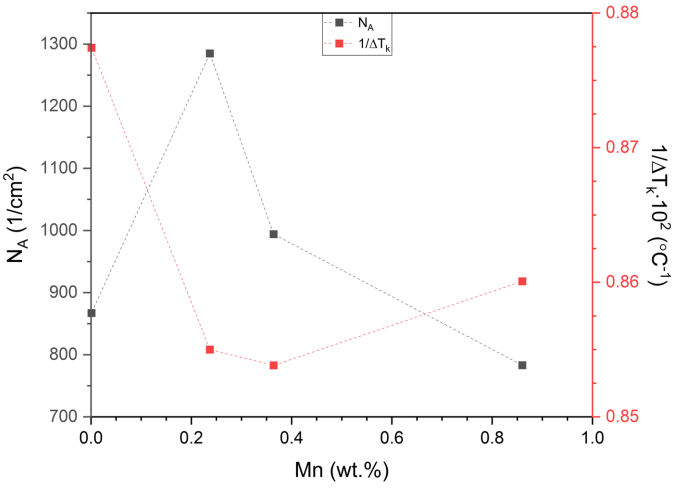

Fig. 12. Number of grains per unit area N_A and $1/\Delta T_k$ as function of variable Mn content for Series III (modified alloy, Ti content of about 0.1 wt.%)

It has been observed that, for Series I (trace Ti content) from a content of about 0.2 wt.% Mn, the number of grains increases and the inverse of the solidification interval decreases (Fig. 10). A different situation occurs for Series II (Ti content of 0.1 wt.%) and Series III (modified alloy containing Ti), where the number of grains decreases for the content above 0.2 wt.% Mn while solidification interval $1/\Delta T_k$ increases (Fig. 11, Fig. 12). These results are consistent with the literature data [11] as to the minimum occurrence for the relationship of the size or number of primary grains and solidification interval $1/\Delta T_k$ as a function of the content of the main alloying element (i.e. silicon in the Al-Si alloys and copper in the Al-Cu alloys). The effect of the minimum $1/\Delta T_k$ visible in Figs. 11 and 12 can be explained by a change in the mechanism of the growth of dendrites or by the influence of titanium [11]. In the case of the interaction of the main alloying elements (i.e. silicon in the Al-Si alloys and copper in the Al-Cu alloys), minimum grain diameter or N_A values occur for the Al-Si and Al-Cu alloys at GRF values of about 5 and 15, respectively (this corresponds to the maximum solubility of a given element) [11]. In the case of the unmodified and titanium-free alloys, there is no minimum $1/\Delta T_k$ (in contrast to the other alloys). This effect can be associated with not exceeding the maximum solubility of Mn in solution α (Al), which is 1.25 wt.% Mn [15]. The addition of titanium increases its concentration in liquid metal, which affects the nucleation process and crystal growth, especially in the presence of boron (Series III).

Research using scanning electron microscope

Fig. 13 shows examples of the EDS test results, which showed the presence of an Al_2Cu phase in the alloy microstructure as well as phases containing Cu, Fe, Mn, and a low Ti content. In point 1 (Fig. 13a) chemical composition is 37 wt.% Cu – 9.6 wt.% Fe – 1.4 wt.% Mn. For Fig. 13b: 19 wt.% Mn – 12.7 wt.% Cu – 4.1 wt.% Fe. For castings with a low content of man-

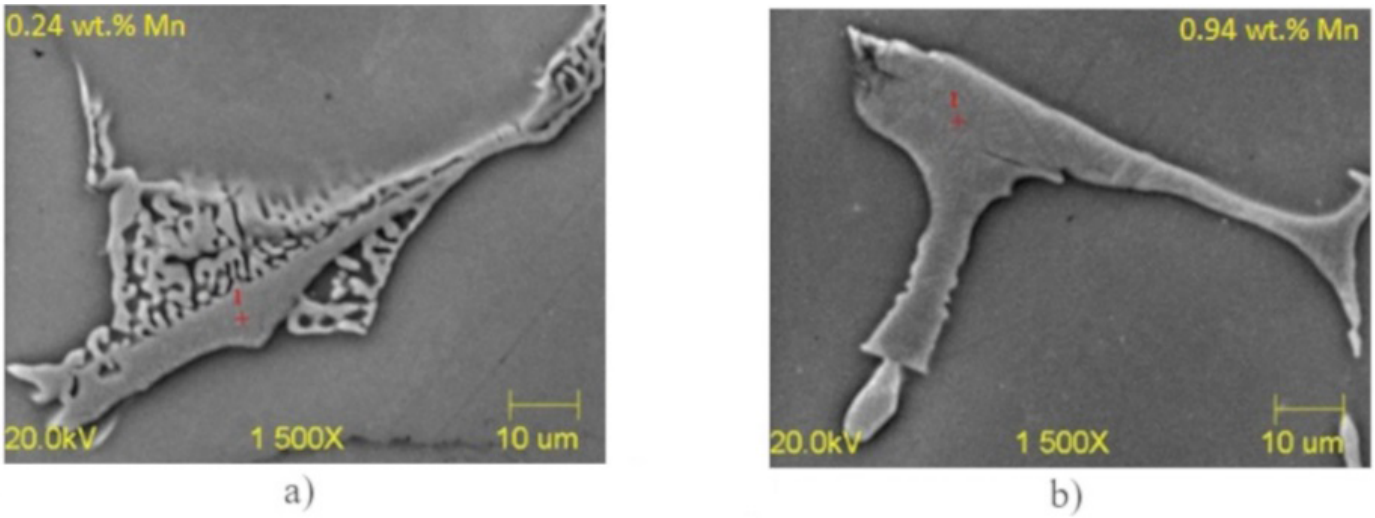

Fig. 13. Microstructure photos taken with scanning microscope with points for chemical composition analysis: a) Series II B; b) Series II D; magnification 1500×

ganese, phases containing Cu, Fe, and Mn in the irregular lamellar shape have been observed in combination with eutectics. In the case of a higher manganese content, there are compact phases.

4. Conclusions

Based on the conducted tests, it was found that the values of the maximum degrees of undercooling ΔT decrease as the Mn content in the alloys increases to a content of 0.4 wt.% Mn, followed by its increase. The addition of Ti at a level of about 0.1 wt.% in the Al-Cu-Mn alloy causes the greatest differences in the maximum degree of undercooling (within a range of 0-0.4 wt.% Mn). A further increase in Mn increases the maximum degree of undercooling.

As the content of manganese increases (from 0.25 wt.%), the number of grains per unit area decreases. High GRF growth restriction factor for titanium indicates its the high impact.

The solidification interval and limiting solubility depend on various factors that affect the physicochemical state and cooling rate. The addition of titanium increases its concentration in the liquid metal, which affects the nucleation process and crystal growth, especially in the presence of boron (Series III).

The EDS studies have shown the presence of Al_2Cu eutectics and phases containing Cu, Fe, Mn, and a low Ti content. At lower manganese contents, these phases appear as irregular lamellar structures, while they have a more compact form at a higher content.

REFERENCES

[1] M. Górny, G. Sikora, E. Tyrała, P. Repeć, Journal of Casting & Materials Engineering **1**, 1, 20-26 (2017), doi: 10.7494/jcme.2017.1.1.20.

[2] M. Guofa, W. Kuangfei, G. Haijun, W. Hongwei, Z. Songyan, China Foundry **5**, 1, 24-27 (2008).

[3] S.M. Dar, H. Liao, A. Xu, J. Alloy Compd. **774**, 758-767 (2019), doi: 10.1016/j.jallcom.2018.09.362.

[4] K. Ren, G. Wang, W. Wang, Y. Hu, H. Wang, Y. Rong, J. Mater. Eng. Perform. **28** (11), 6638-6648 (2019), doi: 10.1007/s11665-019-04441-0.

[5] R.S. Rana, R. Purohit, S. Das, International Journal of Scientific and Research Publications **2** (6), 1-7 (2012).

[6] V.S. Zolotorevsky, N.A. Belov, M.V. Glazoff, Casting Aluminium Alloys, Elsevier (2007).

[7] M.V. Glazoff, A.V. Khvan, V.S. Zolotorevsky, N.A. Belov, A.T. Dinsdale, Casting Aluminium Alloys Their Physical and Mechanical Metallurgy, Butterworth-Heinemann, an Imprint of Elsevier, (2019).

[8] A. Bolouri, X.-Grant Chen, Mater. Sci. Forum **877**, 90-96 (2017) doi: 10.4028/www.scientific.net/MSF.877.90.

[9] K. Liu, X. Cao, X.-G. Chen, Metalurgical and Materials Transaction A **45A**, 2498-2507 (2014), doi: 0.1007/s11661-014-2207-3.

[10] T. Chandrashekar, M.K. Muralidhara, K.T. Kashyap, P. Raghothama Rao, Int. J. Adv. Manuf. Tech., 234-241, (2009), doi: 10.1007/s00170-007-1336-x.

[11] Y. Birol, Int. J. Cast. Metal. Res. **26** (1), 22-27 (2013), doi:10.1179/1743133612Y.0000000023.

[12] D. M. Stefanescu, Science and Engineering of Casting Solidification, Springer International Publishing Switzerland, (2015).

[13] J. Płaczkiewicz, master's thesis, The effect of magnesium on the degree of undercooling and the structure of the Al-5Cu alloy, AGH University of Science and Technology, Krakow (2018) (in Polish).

[14] G. Sikora, Archives of Foundry Engineering **15** (4), 113-118, (2015) (in Polish).

[15] ASM HandBook, Alloy Phase Diagrams **03**, ASM International (1992).